Nonparametric goodness-of fit testing in quantum homodyne tomography with noisy data

Katia Meziani

HAL Id: hal-00311975
https://hal.science/hal-00311975

Submitted on 23 Aug 2008

Nonparametric goodness-of fit testing in quantum homodyne tomography with noisy data

Katia Méziani

email: meziani@math.jussieu.fr

Laboratoire de Probabilités et Modèles Aléatoires,

Université Paris VII (Denis Diderot),

case courier 7012, 2 Place Jussieu 75251 Paris cedex 05, France.

August 23, 2008

Abstract

In the framework of quantum optics, we study the problem of goodness-of-fit testing in a severely ill-posed inverse problem. A novel testing procedure is introduced and its rates of convergence are investigated under various smoothness assumptions. The procedure is derived from a projection-type estimator, where the projection is done in $\mathbb{L}_2$ distance on some suitably chosen pattern functions. The proposed methodology is illustrated with simulated data sets.

1 Introduction

In quantum optics, the results of the measurement of a quantum state ρ are random. Mathematically, a quantum state ρ is entirely characterized by an operator ρ on a complex Hilbert space $\mathcal{H}$ such that ρ is

1. self-adjoint (or Hermitian): $\rho = \rho^*$, where ρ^* is the adjoint of ρ,

2. positive: $\rho \geq 0$, or equivalently $\langle \psi, \rho\psi \rangle \geq 0$ for all $\psi \in \mathcal{H}$,

3. trace one: $\mathrm{Tr}(\rho) = 1$.

In this paper, the studied quantum system is a monochromatic light in a cavity, whose state is described by infinite **density matrices** ρ on the separable Hilbert, hereafter, denoted by $\mathbb{L}_2(\mathbb{R})$, the space of square integrable complex valued functions on the real line. In this setting, a convenient representation of a quantum state can be obtained by the projection onto the orthonormal basis $(\psi_j)_{j \in \mathbb{N}}$, called Fock basis and defined by

$$\psi_j(x) := \frac{1}{\sqrt{\sqrt{\pi} 2^j j!}} H_j(x) e^{-x^2/2}. \tag{1}$$

Here, $H_j(x) := (-1)^j e^{x^2} \frac{d^j}{dx^j} e^{-x^2}$ denotes the j-th Hermite polynomial. Furthermore, to each state ρ corresponds a **Wigner function** W_ρ, which gives an identical representation of the quantum state ρ. The Wigner function is a mapping from $\mathbb{R}^2$ to $\mathbb{R}$ such that $\iint W_\rho(q, p) dq dp = 1$. For this reason, W_ρ is regarded as a generalized joint probability density of the two random variables Q and P that we would get if we could measure simultaneously the two observables $\mathbf{Q}$ and $\mathbf{P}$, which are respectively the electric and the magnetic fields. The Wigner function W_ρ can be defined rigorously by its Fourier transform $\mathcal{F}_2[W_\rho]$ with respect to both variables

$$\widetilde{W}_\rho(u, v) := \mathcal{F}_2[W_\rho](u, v) = \mathrm{Tr}\left(\rho \exp(iu\mathbf{Q} + iv\mathbf{P})\right).$$

In quantum optics, physicists produce quantum state of light and via measurement, they gather independent identically distributed random variables containing information on the unknown, underlying quantum state ρ. The measurements are done

by a technique called quantum homodyne tomography (QHT), which has been put in practice for the first time in [29]. We refer the interested reader to the book [18] or the paper [16] for further details on QHT. Our goal is to check whether the produced light pulse is in the known quantum state τ, or not. This can be done via goodness-of-fit testing. We measure the distance between the unknown state ρ and the presumed state τ by the squared-$\mathbb{L}_2$-distance:

$$\|\rho - \tau\|_2^2 = \sum_{j,k \geq 0} |\rho_{j,k} - \tau_{j,k}|^2 . \tag{2}$$

In an ideal framework, the results of measurement would be $(X_\ell, \Phi_\ell)_{\ell=1,\dots,n}$, independent identically distributed random variables with values in $\mathbb{R} \times [0, \pi]$. Let $p_\rho(x, \phi)$ be the probability density function w.r.t. the measure $\frac{1}{\pi}\lambda$ of (X_1, Φ_1), where λ stands for the Lebesgue measure on $\mathbb{R} \times [0, \pi]$. It is well-known that

$$p_\rho(x|\phi) = \mathcal{R}[W_\rho](x, \phi). \tag{3}$$

Here, $\mathcal{R}$ denotes the Radon transform, taking functions $W_\rho(q, p)$ on $\mathbb{R}^2$ into functions $\mathcal{R}[W_\rho](x, \phi)$ on $\mathbb{R} \times [0, \pi]$ formed by integration along lines of direction ϕ and distance x from the origin, expressed as

$$\mathcal{R}[W_\rho](x, \phi) = \int_{-\infty}^{\infty} W_\rho(x \cos \phi - t \sin \phi, \, x \sin \phi + t \cos \phi) dt.$$

In this paper we consider a more realistic model in presence of an additional independent Gaussian noise. More precisely, we observe $(Y_\ell, \Phi_\ell)_{\ell=1,\dots,n}$ independent identically distributed random variables, given by

$$Y_\ell := \sqrt{\eta} X_\ell + \sqrt{(1-\eta)/2} \, \xi_\ell, \tag{4}$$

where ξ_ℓ is a sequence of independent identically distributed standard Gaussians, independent of all (X_ℓ, Φ_ℓ). The detection efficiency parameter η, $0 < \eta \leq 1$, is a known parameter and $1 - \eta$ represents the proportion of lost photons due to various losses in the measurement process.

The problem of reconstructing the quantum state of a light beam has been extensively studied in quantum statistic and physic literature. Methods for reconstructing a quantum state have been proposed based either on density matrix or on Wigner function estimation. The estimation of the density matrix from averages of data has been considered in the framework of ideal detection [13, 12, 20, 3] as well as in the more general case of an efficiency parameter η belonging to the interval $]1/2, 1]$ (cf. [10, 14, 11, 27]). The case $\eta \in]0, 1]$ has been recently treated in [4]. The latter paper provides also rates of convergence in $\mathbb{L}_2$ loss for an estimator of the Wigner function. The problem of pointwise estimation of the Wigner function has been previously studied in [9] for noisy data and in [16] for ideal data. It should be noted that the results of [16] and most part of the results in [9] are asymptotically minimax not only in the rate, but also in the constant.

In the present work, the goodness-of-fit problem in quantum statistic is considered. There is a large literature on nonparametric testing procedures for the goodness-of-fit of probability distributions. First of all, let us mention the family of test procedures built on certain distances between empirical cumulative distribution functions (c.d.f.), such as the Kolmogorov-Smirnov and the Cramer-Von Mises test statistics, for which extensive results in terms of asymptotic efficiency were established [23]. In order to be more sensitive to low-frequency components or narrow bumps for powerful discrimination, test procedures based on distances between densities were proposed, such as the Bickel-Rosenblatt test [6, 2] for the $\mathbb{L}_2$-distance and the test of [1] for the $\mathbb{L}_1$-distance. Theoretical results on such test statistics naturally stems from their nonparametric function estimation counterparts.

In order to compare nonparametric testing procedures, many approaches were proposed, as reviewed in [23, 17]. A common approach is to analyze the power against sequences of local alternatives $\{f_n\}_{n \geq 1}$ of the form $f_n = f_0 + \varphi_n g$ where g is the direction defining the sequence of local alternatives, and where $\varphi_n \to 0$ as n tends to infinity. Typically, while nonparametric test statistics achieve nontrivial power (i.e. the power of the test is strictly larger than the first type error) against direc-

tional alternatives $f_n = f_0 + \varphi_n g$ when $\varphi_n = Cn^{-1/2}$, they achieve nontrivial power against nondirectional alternatives $f_n = f_0 + \varphi_n g_n$ only for φ_n slower than $n^{-1/2}$. In other words, achieving nontrivial power uniformly against a large class of alternatives comes at the price of a slower rate than for parametric testing. The minimax distinguishability framework described in a non-asymptotic setting in [5, 15] and in an asymptotic setting in [17], allows to give precise statements about this phenomenon by characterizing the discrimination rate φ_n depending on a smoothness index of the class of alternatives one wish to discriminate for the null hypothesis. Sharp minimax results with pointwise and sup-norm distances have been established in [21] for the regression model and in [26] for the Gaussian white noise model for supersmooth functions. In [8], goodness-of-fit testing in the convolution model have been considered and minimax rates for testing in $\mathbb{L}_2$-norm from indirect observations have been established. The first testing procedure adaptive to smoothness of the alternative function was proposed by [30].

In quantum statistic framework, for the problem of discriminating between two different and fixed states we mention [24] among others. They have establish lower bound for the Bayesian error probability.

The remainder of the article is organized as follows. In Section 2, we introduce the notation and define the nonparametric class containing the density matrices we are dealing with. The testing procedure and the theorical results assessing its asymptotic behavior are presented in Section 3. Section 4 contains an illustration of the proposed methodology on simulated data sets while the proof are postponed to Section 5.

2   Preliminaries

For any functions $f, g : \mathbb{R} \to \mathbb{R}$, denote by $f * g$ the convolution product

$$f * g(y) = \int f(y - t)g(t)dt.$$

Since $Y_\ell := \sqrt{\eta} X_\ell + \sqrt{(1 - \eta)/2}\, \xi_\ell$, the density p_ρ^η of (Y_ℓ, Φ_ℓ) is given by the convolution of the density $p_\rho(\cdot / \sqrt{\eta}, \phi)/\sqrt{\eta}$ with N^η the centered Gaussian density of

variance $(1 - \eta)/2$. In other terms

$$p_\rho^\eta(y, \phi) = \left(\frac{1}{\sqrt{\eta}} p_\rho \left(\frac{\cdot}{\sqrt{\eta}}, \phi \right) * N^\eta \right)(y), \quad \forall y \in \mathbb{R}, \ \phi \in [0, \pi].$$

In the Fourier domain, this relation becomes

$$\mathcal{F}_1[p_\rho^\eta(\cdot, \phi)](t) = \mathcal{F}_1[p_\rho(\cdot, \phi)](t\sqrt{\eta})\widetilde{N}^\eta(t), \tag{5}$$

where $\mathcal{F}_1[p_\rho^\eta(\cdot, \phi)]$ denotes the Fourier transform with respect to the first variable and $\widetilde{N}^\eta$ the Fourier transform of the Gaussian density N^η.

We suppose that the unknown state belongs to the class $\mathcal{R}(B, r, L)$ for $B > 0$ and $r \in]0, 2]$ defined by

$$\mathcal{R}(B, r, L) := \{\rho \text{ quantum state} : |\rho_{j,k}| \le L \exp(-B(j + k)^{r/2})\}. \tag{6}$$

This decay condition on the coefficients of the density matrix characterizes both smoothness and the asymptotic behavior of the associated Wigner function. Indeed, it has been translated on the corresponding Wigner function in Proposition 1 and 2 in [4]. Namely, for all $j \ge k$, if $\rho \in \mathcal{R}(B, r, L)$ with $r \in]0, 2[$, then for all $\beta < B$, there exists z_0 (depending explicitly on r, B, β) such that for all (q, p) satisfying $\sqrt{q^2 + p^2} \ge z_0$ we have

$$|W_\rho(q, p)| \le C_r z^{4-r} e^{-\beta z^r}, \tag{7}$$

$$\left|\widetilde{W}_\rho(q, p)\right| \le c_r z^{4-r} e^{-\beta(z/2)^r}, \tag{8}$$

where $z = \sqrt{q^2 + p^2}$. In case where $r = 2$, equations (7) and (8) remain valid for $\beta := \frac{B}{(1+\sqrt{B})^2}$.

Let us consider the problem of nonparametric goodness-of fit testing from the data (Y_ℓ, Φ_ℓ) for $\ell = 1, \ldots, n$. Given $\tau \in \mathcal{R}(B, r, L)$, the physical interpretation of such a test is to check whether the produced light pulse is in a known quantum state τ, or not. This can be done via the density matrix as follows:

$$\begin{cases} H_0 : & \rho = \tau, \\ H_1(\mathcal{C}, \varphi_n) : & \rho \in \mathcal{R}(B, r, L) \text{ such that } \|\rho - \tau\|_2 \ge \mathcal{C} \cdot \varphi_n, \end{cases}$$

where φ_n is a sequence, which tends to 0 when $n \to \infty$.

Definition 1. *For a given $0 < \lambda < 1$, a test procedure Ω_n satisfies the upper bound (9) for the testing rate φ_n over the smoothness class $\mathcal{R}(B, r, L)$ if there exists a constant $\mathcal{C}^* > 0$ such that for all $\mathcal{C} > \mathcal{C}^*$:*

$$\limsup_{n \to \infty} \left\{ P_\tau[\Omega_n = 1] + \sup_{\rho \in H_1(\mathcal{C}, \varphi_n)} P_\rho[\Omega_n = 0] \right\} \leq \lambda, \tag{9}$$

where P_τ denote the probability under $\rho = \tau$ defined in H_0.

We present in Table 1 examples of pure quantum states, which can be created at this moment in laboratory and belong to the class $\mathcal{R}(B, r, L)$ with $r = 2$. A state is called pure if it cannot be represented as a mixture (convex combination) of other states, i.e., if it is an extreme point of the convex set of states. This is equivalent to the density matrix being a one dimensional projector, i.e., of the form $\rho = \mathbf{P}_\psi$ for some unit vector ψ. In this case the formula for the expectation value of an operator A in the state simplifies as $tr(A\rho) = E_\rho[A]$. Equivalently, a state ρ is pure if $\mathrm{Tr}(\rho^2) = 1$. All other states are called mixed states.

Let us discuss these few examples of quantum states. Among the pure states we consider the *single photon* state and the *vacuum* state, which is the pure state of zero photons. Note that the *vacuum* state would provide a random variable of Gaussian probability density $p_\rho(x|\phi)$ via the ideal measurement of quantum homodyne tomography.. We consider also the *coherent-q_0* state, which characterizes the laser pulse with the number of photons Poisson distributed with an average of M photons. The *Squeezed* states (see e.g. [7]) have Gaussian Wigner functions whose variances in the two directions have a fixed product. The parameters M and ξ are such that $M \geq \sinh^2(\xi)$, $C(M, \xi)$ is a normalization constant, $\alpha = \frac{(M - \sinh^2(\xi))^{1/2}}{\cosh(\xi) - \sinh(\xi)}$, and $\delta = \left(\frac{\alpha}{\sinh(2\xi)}\right)^{1/2}$. The well-known *Schrödinger cat* state is described by a linear superposition of two *coherent* vectors (see e.g. [25]). Table 1 gives some explicit density matrix coefficients $\rho_{j,k}$ and probability densities $p_\rho(x|\phi)$.

Table 1: Examples of quantum states

Vacuum state
• $\rho_{0,0} = 1$ rest zero,
• $p_\rho(x\|\phi) = e^{-x^2}/\sqrt{\pi}$.
Single photon state
• $\rho_{1,1} = 1$ rest zero,
• $p_\rho(x\|\phi) = 2x^2 e^{-x^2}/\sqrt{\pi}$.
Coherent-q_0 state $q_0 \in \mathbb{R}$
• $\rho_{j,k} = e^{-\|q_0\|^2} q_0^{j+k}/\sqrt{j!k!}$,
• $p_\rho(x\|\phi) = \exp(-(x - q_0\cos(\phi))^2)/\sqrt{\pi}$.
Squeezed state $M \in \mathbb{R}_+,\ \xi \in \mathbb{R}$
• $\rho_{j,k} = C(M,\xi)(\frac{1}{2}\tanh(\xi))^{k+j} H_j(\delta) H_k(\delta)/\sqrt{j!k!}$,
• $p_\rho(x\|\phi) = \exp\left[\left(\sin^2(\phi)(xe^{-2\xi}\cos(\phi) - (x\cos(\phi) - \alpha)e^{2\xi})^2\right) \big/ \left(e^{2\xi}\sin^2(\phi) + e^{-2\xi}\cos^2(\phi)\right)\right.$ $\left. \times\, -e^{-2\xi}(x\cos(\phi) - \alpha)^2 - e^{2\xi}x^2\sin^2(\phi)\right] \big/ \sqrt{\pi(e^{2\xi}\sin^2(\phi) + e^{-2\xi}\cos^2(\phi))}$.
Thermal state $\beta > 0$
• $\rho_{j,k} = \delta_k^j (1 - e^{-\beta})e^{-\beta k}$,
• $p_\rho(x\|\phi) = \sqrt{\tanh(\beta/2)/\pi}\,\exp(-x^2\tanh(\beta/2))$.
Schrödinger cat $q_0 > 0$
• $\rho_{j,k} = 2(q_0/\sqrt{2})^{j+k} \big/ \left(\sqrt{j!k!}(\exp(q_0^2/2) + \exp(-q_0^2/2))\right)$, for j and k even, rest zero,
• $p_\rho(x\|\phi) = (\exp(-(x - q_0\cos(\phi))^2) + \exp(-(x + q_0\cos(\phi))^2)$ $+ 2\cos(2q_0 x\sin(\phi))\exp(-x^2 - q_0^2\cos^2(\phi))) \big/ (2\sqrt{\pi}(1 + \exp(-q_0^2)))$.

3 Testing Procedure and results

In the setting described in previous sections, we provide in this part our test from a projection method on pattern functions and we establish our main theorical results. Let us first define the pattern functions and derive some useful properties.

3.1 Pattern functions

First introduced in [20], the *pattern functions* $f_{j,k}$ for $j \geq k$ are functions well known in physic defined in [19] as the first derivatives of products of the functions ψ_k and φ_k,

$$f_{j,k}(x) = \frac{\partial}{\partial x} \left(\psi_j(x) \varphi_k(x) \right).$$

The functions ψ_k and φ_k are the two fundamental solutions of the Schrödinger equation

$$\left[-\frac{1}{2} \frac{\partial^2}{\partial x^2} + \frac{x^2}{2} \right] \psi = w\psi, \qquad w \in \mathbb{R},$$

for a given frequency w_k. The function ψ_k is the normalized function as $\int \psi_k^2 = 1$ for an eigenvalues w_k. The function ψ_k is called the regular wave function, while the function φ_k is called the irregular one as it cannot be normalizable as ψ_k is.

The matrix elements $\rho_{j,k}$ of the state ρ in the Fock basis can be expressed as expected values of the functions $F_{j,k}(X_\ell, \Phi_\ell) = f_{j,k}(X_\ell)e^{-i(k-j)\Phi_\ell}$, where $f_{j,k} = f_{k,j}$ are bounded real pattern functions [18],.i.e. for all $j, k \in \mathbb{N}$,

$$\rho_{j,k} = \iint_0^\pi p_\rho(x, \phi) f_{j,k}(x) e^{-i(k-j)\phi} d\phi dx.$$

In others words

$$\rho_{j,k} = E_\rho \left[F_{j,k}(X_\ell, \Phi_\ell) \right]. \tag{10}$$

Equation (10) expresses the idea that one can reconstruct any density matrix element $\rho_{j,k}$ from the knowledge of the pattern functions.

A concrete expression for their Fourier transform using generalized Laguerre polynomials can be found in [28], [4]. For $j \geq k$

$$\tilde{f}_{j,k}(t) = \pi(-i)^{j-k}\sqrt{\frac{2^{k-j}k!}{j!}}|t|t^{j-k}e^{-\frac{t^2}{4}}L_k^{j-k}(\frac{t^2}{2}), \tag{11}$$

where $\tilde{f}_{j,k}$ denotes the Fourier transform of the Pattern function $f_{j,k}$ and $L_k^{\alpha}(x)$ denotes the generalized Laguerre polynomial.

We can note that the pattern functions $f_{j,k}(x)$ are even functions for even differences $j - k$ and odd functions for odd ones

$$f_{j,k}(-x) = (-1)^{j-k}f_{j,k}(x).$$

To take into account the detection losses described by the overall efficiency η, it is necessary to adapt the pattern functions. When $\eta \in]1/2, 1]$, we denote by $f_{j,k}^{\eta}$ the function introduced in [4] and defined by their Fourier transform as follows:

$$\tilde{f}_{j,k}^{\eta}(t) := \tilde{f}_{j,k}(t)e^{\frac{1-\eta}{4\eta}t^2}. \tag{12}$$

In this paper we develop a procedure for $\eta \in]1/2, 1]$, but it is possible to get quite similar results with the same procedure for $0 < \eta \leq \frac{1}{2}$ by using modified pattern functions, those introduced in [4]. We restrict our study to the more interesting case $\eta \in]1/2, 1]$ as in practice η is around 0.9. The following lemma provides useful upper bounds on the $\mathbb{L}_2$-norm of the $f_{j,k}$ and the $\mathbb{L}_{\infty}$-norm of the $f_{j,k}^{\eta}$. From now on, we denote $\gamma := \frac{1-\eta}{4\eta}$.

Lemma 1 (Aubry *et al.* [4]). *There exists a constant $\mathcal{C}_2$ such that for N large enough*

$$\sum_{j,k=0}^{N}\|f_{j,k}\|_2^2 \leq \mathcal{C}_2 N^{\frac{17}{6}}.$$

For $\eta \in]1/2, 1[$ and $\gamma = \frac{1-\eta}{4\eta}$, there exists constant $\mathcal{C}_{\infty}^{\eta}$ such that for N large enough

$$\sum_{j,k=0}^{N}\left\|f_{j,k}^{\eta}\right\|_{\infty}^2 \leq \mathcal{C}_{\infty}^{\eta}N^{-\frac{2}{3}}e^{16\gamma N}.$$

For the $\mathbb{L}_{\infty}$-norm of the $f_{j,k}^{\eta}$, this lemma is slightly different from Lemmata 4 and 5 in [4] where the sum is over $j + k = 0, \ldots, N$. The proof remains similar.

10

3.2 Testing procedure

In this section we derive an estimator of $\|\rho - \tau\|_2^2$ based on indirect observations $(Y_i, \Phi_i)_{i=1,\dots,n}$ and study its properties. We provide our test procedure for $\eta \in]1/2, 1]$.

For $\eta \in]1/2, 1]$, $N := N(n) \to \infty$ and $\delta := \delta(n) \to 0$, let us define an estimator M_n of $\|\rho - \tau\|_2^2$ as an U-statistic of order 2 by

$$M_n := \frac{1}{n(n-1)} \sum_{j,k=0}^{N-1} \sum_{\ell \neq m=1}^{n} \left[F_{j,k}^{\eta}\left(\frac{Y_\ell}{\sqrt{\eta}}, \Phi_\ell\right) - \tau_{j,k} \right] \left[\overline{F_{j,k}^{\eta}}\left(\frac{Y_m}{\sqrt{\eta}}, \Phi_m\right) - \overline{\tau_{j,k}} \right], \quad (13)$$

where

$$F_{j,k}^{\eta}(x, \phi) := f_{j,k}^{\eta}(x) e^{-i(k-j)\phi} \mathbb{1}_{\{0 \leq j,k \leq N-1\}}$$

uses the pattern functions defined in (12) and $\overline{a}$ denote the complex conjugate of a.

For the test statistic M_n defined in (13), a constant $\mathcal{C} > 0$ and some threshold $t_n > 0$, we define the test procedure as

$$\Omega_n = \mathbb{1}(|M_n| > \mathcal{C} \cdot t_n^2). \quad (14)$$

We first remark that each element of the density matrix is estimated with no bias. Moreover, the estimator M_n is unbiased under $\rho = \tau$ defined in H_0 (Remark 1). Remark 2 relates useful tools for the proof of the upper bounds in the sense of Definition 1. From now on, we denote by E_ρ the expected value under ρ satisfying $H_1(\mathcal{C}, \varphi_n)$ and E_τ under $\rho = \tau$ defined in H_0.

Remark 1. *Note that for $0 \leq k \leq j \leq N-1$ and $\eta \in]1/2, 1]$*

$$E_\rho \left[F_{j,k}^{\eta}\left(\frac{Y}{\sqrt{\eta}}, \Phi\right) \right] = \rho_{j,k} \quad and \quad E_\tau \left[F_{j,k}^{\eta}\left(\frac{Y}{\sqrt{\eta}}, \Phi\right) \right] = \tau_{j,k}.$$

11

Indeed, from Plancherel formula

$$E_\rho \left[F_{j,k}^\eta \left(\frac{Y}{\sqrt{\eta}}, \Phi \right) \right] = \iint_0^\pi \int f_{j,k}^\eta(\frac{y}{\sqrt{\eta}}) e^{-i(k-j)\phi} p_\rho^\eta(y, \phi) d\phi dy$$

$$= \iint_0^\pi f_{j,k}^\eta(y) e^{-i(k-j)\phi} \sqrt{\eta} p_\rho^\eta(\sqrt{\eta} y, \phi) d\phi dy$$

$$= \iint_0^\pi e^{-i(k-j)\phi} \frac{1}{2\pi} \tilde{f}_{j,k}(t) e^{\frac{1-\eta}{4\eta} t^2} \mathcal{F}_1[\sqrt{\eta} p_\rho^\eta(\cdot \sqrt{\eta}, \phi)](t) d\phi dt.$$

From equation (5), and from Plancherel formula

$$E_\rho \left[F_{j,k}^\eta \left(\frac{Y}{\sqrt{\eta}}, \Phi \right) \right] = \iint_0^\pi \frac{e^{-i(k-j)\phi}}{2\pi} \tilde{f}_{j,k}(t) e^{\frac{1-\eta}{4\eta} t^2} \mathcal{F}_1[p_\rho(\cdot, \phi)](t) \widetilde{N}^\eta(t/\sqrt{\eta}) d\phi dt$$

$$= \iint_0^\pi e^{-i(k-j)\phi} f_{j,k}(x) p_\rho(x, \phi) d\phi dx = \rho_{j,k}.$$

Thus,

$$E_\rho \left[M_n \right] = \sum_{j,k=0}^{N-1} \left(\rho_{j,k} - \tau_{j,k} \right)^2 \quad and \quad E_\tau \left[M_n \right] = 0.$$

Remark 2. *For N large enough and ρ belonging to the class $\mathcal{R}(B, r, L)$*

$$\sum_{j,k=0}^{N-1} E_\rho \left[\left| F_{j,k}^\eta \left(\frac{Y}{\sqrt{\eta}}, \Phi \right) \right|^2 \right] \leq \begin{cases} \mathcal{C}_\infty^\eta N^{-2/3} e^{16\gamma N} & \eta \in]1/2, 1[, \\ C \cdot \mathcal{C}_2 N^{17/6} & \eta = 1, \end{cases}$$

where $\mathcal{C}_\infty^\eta$ and $\mathcal{C}_2$ are constants defined in Lemma 1 and C is a positive constant.

Proof. Since $E_\rho \left[\left| F_{j,k}^\eta \left(\frac{Y}{\sqrt{\eta}}, \Phi \right) \right|^2 \right] = E_\rho \left[\left| f_{j,k}^\eta \left(\frac{Y}{\sqrt{\eta}}, \Phi \right) \right|^2 \right]$ For $\eta \in]1/2, 1]$

$$\sum_{j,k=0}^{N-1} E_\rho \left[\left| F_{j,k}^\eta \left(\frac{Y}{\sqrt{\eta}}, \Phi \right) \right|^2 \right] \leq \begin{cases} \sum_{j,k=0}^{N-1} \left\| f_{j,k}^\eta \right\|_\infty^2 & \eta \in]1/2, 1[, \\ C \sum_{j,k=0}^{N-1} \left\| f_{j,k}^\eta \right\|_2^2 & \eta = 1. \end{cases}$$

For $\eta = 1$, we first apply Lemma 6 in [4] where it has been established that

$$\sup_{x \in \mathbb{R}} \int_0^\pi p_\rho(x, \phi) d\phi \leq C,$$

where C is a positive constant. Hence, the result is a direct consequence of Lemma 1.

$\square$

In order to choose optimal the bandwidth N, we do the classical bias/variance trade-off. Hence, the following Propositions evaluate under $\rho = \tau$ defined in H_0 and under ρ satisfying $H_1(\mathcal{C}, \varphi_n)$, the bias term $B_\tau(M_n) := |E_\tau[M_n]|$ and $B_\rho(M_n) := |E_\rho[M_n] - \|\rho - \tau\|_2^2|$ (Proposition 1) and the variance term $V_\tau := E_\tau\left[|M_n - E_\tau[M_n]|^2\right]$ and $V_\rho := E_\rho\left[|M_n - E_\rho[M_n]|^2\right]$ (Proposition 2).

Proposition 1. *For $r \in]0, 2]$, and $\eta \in]1/2, 1]$ we have*

- *under $\rho = \tau$ defined in H_0, $B_\tau(M_n) = 0$,*

- *under ρ satisfying $H_1(\mathcal{C}, \varphi_n)$, for N large enough*

$$B_\rho(M_n) \leq C_B N^{2-r/2} e^{-2BN^{r/2}},$$

  where C_B is a positive constant depending only on B, r and L.

Proposition 2. *For $r \in]0, 2]$ and $\gamma = \frac{1-\eta}{4\eta}$ we have for N large enough*

- *under ρ satisfying $H_1(\mathcal{C}, \varphi_n)$, $\eta = 1$ and for N s.t. $\frac{N^{17/6}}{n} \to 0$ as $n \to \infty$,*

$$V_\rho(M_n) \leq \frac{8C \cdot \mathcal{C}_2}{n} N^{17/6},$$

- *under ρ satisfying $H_1(\mathcal{C}, \varphi_n)$, $\eta \in]1/2, 1[$ and for N s.t. $\frac{N^{-2/3}}{n} e^{16\gamma N} \to 0$ as $n \to \infty$*

$$V_\rho(M_n) \leq \frac{8\mathcal{C}_\infty^\eta N^{-2/3}}{n} e^{16\gamma N},$$

- *and under $\rho = \tau$ defined in H_0, $\eta = 1$ and for N s.t. $\frac{N^{17/6}}{n} \to 0$ as $n \to \infty$,*

$$V_\tau(M_n) \leq \frac{(C \cdot \mathcal{C}_2)^2}{n^2} N^{17/3},$$

- *and under $\rho = \tau$ defined in H_0, $\eta \in]1/2, 1[$ and for N s.t. $\frac{N^{-2/3}}{n} e^{16\gamma N} \to 0$ as $n \to \infty$.*

$$V_\tau(M_n) \leq \frac{(\mathcal{C}_\infty^\eta)^2 N^{-4/3}}{n^2} e^{32\gamma N},$$

The constants $\mathcal{C}_\infty^\eta$ and $\mathcal{C}_2$ are defined in Lemma 1 and C is positive constant.

3.3 Main results

In the following Theorem, we establish upper bounds in the sense of Definition 1 where ρ is the unknown density matrix supposed to belong to the class $\mathcal{R}(B, r, L)$ defined in (6). Theorem 1-(1) deals with the ideal detection case while Theorem 1-(2) and Theorem 2 take into account the Gaussian noise.

Theorem 1. *The test procedure Ω_n defined in (14) for the bandwidth $N(n)$, the threshold t_n and the constant $\mathcal{C}^*$ satisfies the upper bound (9) for the rate φ_n such that*

1. *for $r \in]0, 2]$, $\eta = 1$, the bandwidth $N(n) := N_1$ is equal to*

$$N_1 := \left(\frac{\log n}{4B} + \frac{(\log \log n)^2}{4B} \right)^{2/r},\tag{15}$$

  and the rate

$$\varphi_n^2 = t_n^2 = n^{-1/2} (\log n)^{\frac{17}{6r}},\tag{16}$$

2. *for $r = 2$, $\eta \in]1/2, 1[$ and $\gamma := \frac{1-\eta}{4\eta}$, the bandwidth $N(n) := N_2$ is equal to*

$$N_2 := \frac{\log(n)}{4(4\gamma + B)} \left(1 + \frac{8}{3} \frac{\log(\log n)}{\log(n)} \right),\tag{17}$$

  and the rate

$$\varphi_n^2 = t_n^2 = \log(n)^{\frac{12\gamma - B}{3(4\gamma + B)}} n^{-\frac{B}{2(4\gamma + B)}}.\tag{18}$$

Theorem 2. *For $r \in]0, 2[$, $\eta \in]1/2, 1[$ and $\gamma = \frac{1-\eta}{4\eta}$, the test procedure Ω_n defined in (14) for the bandwidth $N := N_3$ solution of the equation*

$$16\gamma N_3 + 4B N_3^{r/2} = \log n,\tag{19}$$

the threshold t_n and the constant $\mathcal{C}^*$ satisfies the upper bound (9) for the rate φ_n

$$\varphi_n^2 = t_n^2 = N_3^{2-r/2} e^{-2B N_3^{r/2}}.\tag{20}$$

We can remark that

$$\limsup_{n \to \infty} \left\{ P_\tau[\Omega_n = 1] + \sup_{\rho \in H_1(\mathcal{C}, \varphi_n)} P_\rho[\Omega_n = 0] \right\} = 0.$$

Theorem 1 and 2 provide upper bounds for our testing procedure defined in equation (14) for the testing rates φ_n. We first remark that our procedure gives nearly parametric rate up to a logarithmic factor since we are in the framework of ideal detection (no noise) and supersmooth corresponding Wigner functions for all $r \in]0,2]$. In the setting of Theorem 1-(2) and Theorem 2, there are good reasons to believe that our testing procedure achieves optimal rates. This remark follows from a recent work of Butucea ([8]), where the author establishes minimax rates for testing in $\mathbb{L}_2$-norm from indirect observations. However, we do not attempt to go that far in this paper.

The point of this paper is the study in a nonparametric setup of the properties of goodness-of-fit testing by a procedure based on a projection estimator on pattern functions. In order to compare our procedure in the framework of quantum statistic, one can investigate a new approach based on kernel type estimation. Such a testing procedure can been directly derived from the kernel estimator in [22] of the quadratic functional $\iint W_\rho^2$, where W_ρ is the Wigner function associated to the quantum state ρ. Our test problem is equivalent to the following:

$$\begin{cases} H_0: & W_\rho = W_{\rho_0}, \\ H_1: & \sup_{\rho \in \mathcal{R}(B,r,L)} \|W_\rho - W_{\rho_0}\|_2 \geq \mathcal{C} \cdot \varphi_n \end{cases}$$

where φ_n is a sequence which tends to 0 when $n \to \infty$. We conjecture that its performances are comparable to those found in this paper and we will leave this analysis for a separate work.

4 Simulations

From now on, we set $r = 2$. The purpose of this Section 4 is to implement our testing procedure and to investigate its numerical performances. Our motivation is, given a

density matrix $\tau \in \mathcal{R}(B, r)$, to decide whether H_0 or H_1 is accepted

$$\begin{cases} \quad H_0: \quad\quad \rho = \tau, \\ H_1(\mathcal{C}, \varphi_n): \quad \rho \in \mathcal{R}(B, r, L) \text{ s.t. } \|\rho - \tau\|_2 \geq \mathcal{C} \cdot \varphi_n, \end{cases}$$

where φ_n is a sequence, which tends to 0 when $n \to \infty$. We propose to simulate two different situations. In the first one, case **A**, we consider quantum states easily distinguishable, while in the second one, case **B**, we deal with quantum states, which are quite similar and it is difficult to differentiate between them. For τ defined in H_0, we sample our procedure from different density matrices ρ satisfying $H_1(\mathcal{C}, \varphi_n)$ such that in

- the case **A**: τ is the *vacuum* state, while

  - **a)** ρ is the *vacuum* state ($\rho = \tau$),

  - **b)** ρ is the *single photon* state,

  - **c)** ρ is the *Schrödinger cat* state,

- the case **B**: τ is the *coherent*-3 state, while

  - **a)** ρ is the *coherent*-3 state ($\rho = \tau$),

  - **b)** ρ is the *coherent*-$\sqrt{6}$ state,

  - **c)** ρ is the *Schrödinger cat* state.

The latter case is a more complicated situation for two main reasons. The *Schrödinger cat* state corresponds to a linear superposition of two *coherent* states ($\pm q_0$). Moreover, the probability density of a *coherent*-q_0 state is Gaussian with a mean proportional to q_0 (see Table 1). Figures 1 to 3 represent the density matrices of the states we consider in our simulations.

In each situation (cases **A** and **B**), we shall consider the case $\eta = 1$, which corresponds to the ideal detection and the case $\eta = 0.9$ i.e. when noise is present. The latter case is the practical one in laboratory. From now on, we set that:

- for $\eta = 1$, $N = 15$ in both situations,

- for $\eta = 0.9$ and in both situations we consider two different values for N

  - $N = 14$

  - $N = 13$.

We can notice that, when we are in presence of noise ($\eta = 0.9$), we have to take N smaller than the one we choose in the ideal setting. It can be explained by the fact that the variance term of our estimator increase exponentially with N in the case $\eta = 0.9$ (see Proposition 2).

In every experiments, each trial is designed as follows. We sample $n = 50000$ i.i.d. data from each of the three probability densities p_ρ defined in Table 1 for ρ chosen as above. The Gaussian noise component ξ is simulated independently with a variance equals to $\sqrt{(1 - \eta)/2}$. We run several iterations and denote by n_e the number of iterations.

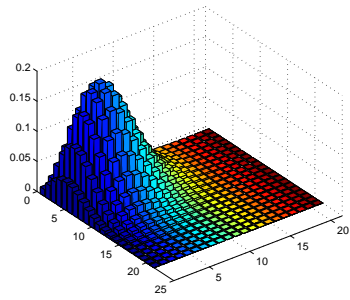Figure 1: Density matrices of the states considered in the case **A**
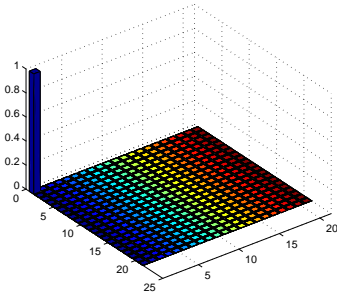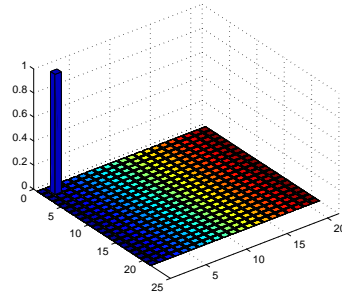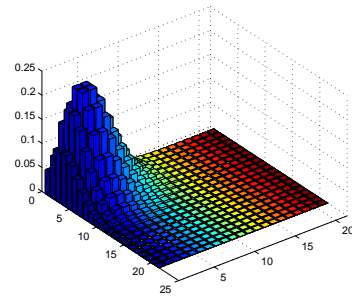

(a) The *vacuum* state   (b) The *single photon* state

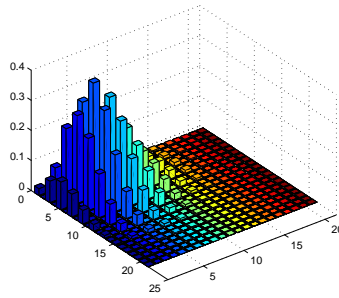Figure 2: Density matrices of the states considered in the case **B**

(a) The *coherent*-3 state

(b) The *coherent*-$\sqrt{6}$ state

Figure 3: Density matrices of the states considered in both cases **A** and **B**

(a) The *Schrödinger cat* state for
$q_0 = 3$

To implement our procedure, we compute our modified pattern function $f_{j,k}^{\eta}(x)$ in Section 4.1. We implement in Section 4.2 the estimator M_n defined in (13) and finally, we study the performance of our test procedure Ω_n defined in (14) in Section 4.3.

4.1 Pattern functions $f_{j,k}^{\eta}$

To illustrate our procedure, we need the modified pattern function $f_{j,k}^{\eta}(x)$ defined in (12) for all $j \geq k$. For this purpose, we compute here the inverse Fourier Transform $f_{j,k}^{\eta}(x)$ of the $\tilde{f}_{j,k}^{\eta}(t)$ given esplicitly by (12) and the generalized Laguerre polynomials. Previous authors have used different method to implement the pattern function in [19, 3] via a following recurrence relations defined in [18]:

$$f_{j,k}(x) = 2x\psi_k(x)\varphi_j(x) - \sqrt{2(k+1)}\psi_{k+1}(x)\varphi_j(x) - \sqrt{2(j+1)}\psi_k(x)\varphi_{j+1}(x),$$

for $j \geq k$, otherwise $f_{j,k}(x) = f_{k,j}(x)$. We display in Figure 4 the corresponding graphical representations of the pattern functions up to a constant π as in physic literature $\pi^{-1}f_{j,k}$ instead of $f_{j,k}$ are often called pattern functions. Figure 5 represents some modified pattern functions $\pi^{-1}f_{j,k}^{\eta}$ for $\eta = 0.9$.

For some of $f_{j,k}$ we expressed below their explicit form.

$$f_{0,0}(x) = 2 - 2e^{-x^2}x\sqrt{\pi}\mathtt{Erfi}(x),$$

$$f_{2,1}(x) = e^{-x^2}\left[-2e^{x^2}x(-3+2x^2) + \sqrt{\pi}(1-8x^2+4x^4)\mathtt{Erfi}(x)\right],$$

$$f_{4,2}(x) = \frac{e^{-x^2}}{2\sqrt{3}}\left[2e^{x^2}\left(-4+27x^2-24x^4+4x^6\right)\right.$$
$$\left.+\sqrt{\pi}x\left(21-74x^2+52x^4-8x^6\right)\mathtt{Erfi}(x)\right],$$

$$f_{5,5}(x) = \frac{e^{-x^2}}{30}\left[2e^{x^2}\left(-30+435x^2-865x^4+526x^6-116x^8+8x^{10}\right)\right.$$
$$\left.+\sqrt{\pi}x\left(225-1425x^2+2160x^4-1160x^6+240x^8-16x^{10}\right)\mathtt{Erfi}(x)\right].$$
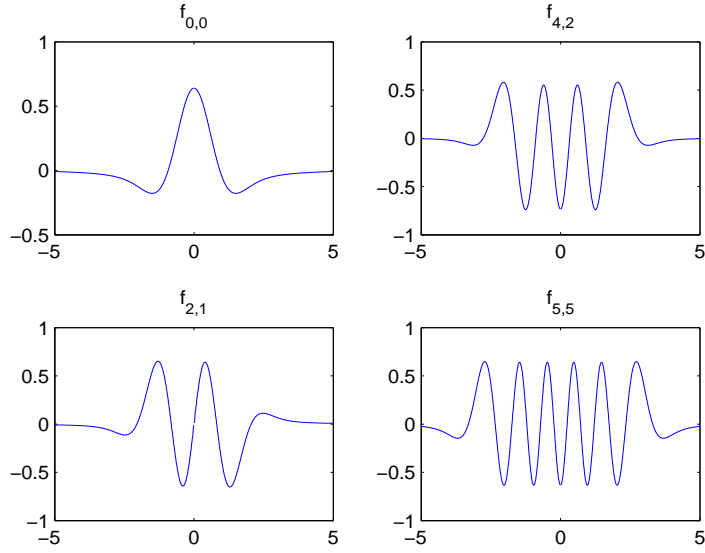
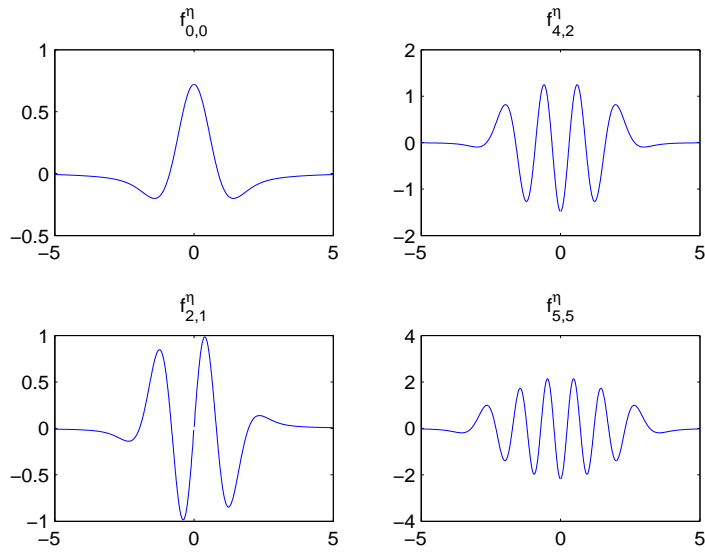Figure 4: Examples of pattern functions $f_{j,k} = f_{j,k}^{\eta}$ for $\eta = 1$

Figure 5: Examples of pattern functions $f_{j,k}^{\eta}$, $\eta = 0.9$

4.2 Implementation of M_n

The purpose of this Section 4.2 is to investigate the performance of the estimator M_n. We recall that M_n is defined as follows:

$$M_n = \frac{1}{n(n-1)} \sum_{j,k=0}^{N-1} \sum_{\ell \neq m=1}^{n} \left[F_{j,k}^{\eta}\left(\frac{Y_\ell}{\sqrt{\eta}}, \Phi_\ell\right) - \tau_{j,k} \right] \left[\overline{F_{j,k}^{\eta}}\left(\frac{Y_m}{\sqrt{\eta}}, \Phi_m\right) - \overline{\tau_{j,k}} \right],$$

where $F_{j,k}^{\eta}(x,\phi) = f_{j,k}^{\eta}(x)e^{-i(k-j)\phi}\mathbb{1}_{\{0 \leq k \leq j \leq N-1\}}$ and τ is defined in H_0. From now on, every values of M_n shall be based on $n = 50000$ i.i.d noisy data (Y_ℓ, Φ_ℓ). The procedure M_n is an estimator of the $\mathbb{L}_2$ distance $\|\rho - \tau\|_2^2 = \sum_{j,k=0}^{N-1}(\rho_{j,k} - \tau_{j,k})^2$ and in our case we project onto the space of matrices of dimension $N = N(n)$ with respect to the basis $\{\psi_k\}_{k=0}^{\infty}$. We are interested in the true values of $\|\rho - \tau\|_2^2$ in the different cases, Table 2 and 3 give the values of $\|\rho - \tau\|_2^2$. We recall that the choice of $N = 15$ corresponds to the setting of ideal detection with $\eta = 1$, while $N = 14$ and $N = 13$ deal with the noisy detection with $\eta = 0.9$. Note that for $\rho = \tau$ we expect M_n to be close to 0 while for ρ satisfying $H_1(\mathcal{C}, \varphi_n)$ we expect M_n to be close to $\|\rho - \tau\|_2^2$.

Table 2: The values of $\|\rho - \tau\|_2^2)$ for case **A**: τ the *vacuum* state

ρ	**a)** *vacuum*	**b)** *single photon*	**c)** *Schrödinger cat*
0		2	1.9556

Table 3: The values of $\|\rho - \tau\|_2^2$ for case **B**: τ the *coherent-3* state

ρ	**a)** *coherent-3*	**b)** *coherent-$\sqrt{6}$*	**c)** *Schrödinger cat*
0		0.2812	0.9999

We run $n_e = 1000$ iterations of M_n in each situation in framework **A** and in framework **B**. Table 4 and 5 summarize the median values. We see in these experiments that our estimator M_n :

- in the setting **A**: M_n is almost $\|\rho - \tau\|_2^2 = 0$ when $\rho = \tau$ and is close to the true value $\|\rho - \tau\|_2^2$ otherwise either for $\eta = 1$ or $\eta = 0.9$,

- in the setting **B**: when $\rho = \tau$, the procedure M_n shows excellent results since M_n is close to $\|\rho - \tau\|_2^2 = 0$ either when $\eta = 1$ or $\eta = 0.9$. In the ideal case and when ρ is the *coherent*-$\sqrt{6}$ state, the procedure M_n gives a good result since the median of the boxplot of M_n is equal to 0.2688 and the true value $\|\rho - \tau\|_2^2 = 0.2812$. Otherwise, the procedure M_n under evaluates the distance $\|\rho - \tau\|_2^2$.

Table 4: The medians for case **A**: τ the *vacuum* state

ρ	**a)** *vacuum*	**b)** *single photon*	**c)** *Schrödinger cat*
$N = 15, \eta = 1$	0.0043	1.9972	1.9417
$N = 14, \eta = 0.9$	0.0256	1.9936	1.9360
$N = 13, \eta = 0.9$	0.0144	1.9943	1.9378

Table 5: The medians for case **B**: τ the *coherent*-3 state

ρ	**a)** *coherent*-3	**b)** *coherent*-$\sqrt{6}$	**c)** *Schrödinger cat*
$N = 15, \eta = 1$	$-6.8721 \cdot 10^{-4}$	0.2688	0.8962
$N = 14, \eta = 0.9$	-0.0466	0.1704	0.7735
$N = 13, \eta = 0.9$	-0.0376	0.1847	0.7840

Figure 6 to 11 show boxplot of $n_e = 1000$ values of the estimator M_n in each experiment.

Figure 6: Case **A** τ is the *vacuum* state: **a)** ρ the *vacuum* state, **b)** ρ the *single photon* state and **c)** ρ the *Schrödinger cat* state for $\eta = 1$, $N = 15$

Figure 7: Case **A** τ is the *vacuum* state: **a)** ρ the *vacuum* state, **b)** ρ the *single photon* state and **c)** ρ the *Schrödinger cat* state for $\eta = 0.9$, $N = 14$
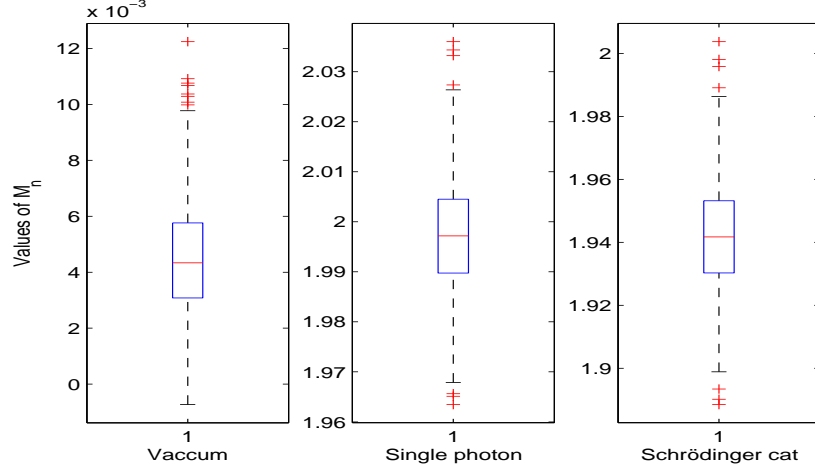
Figure 8: Case **A** τ is the *vacuum* state: **a)** ρ the *vacuum* state, **b)** ρ the *single photon* state and **c)** ρ the *Schrödinger cat* state for $\eta = 0.9$, $N = 13$
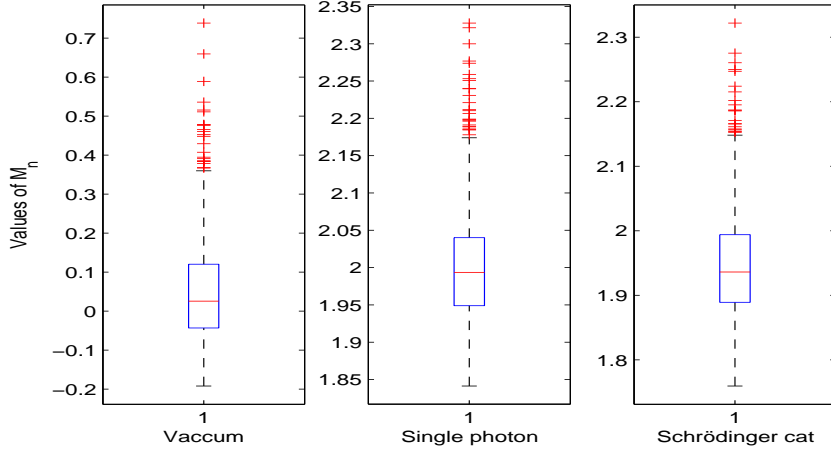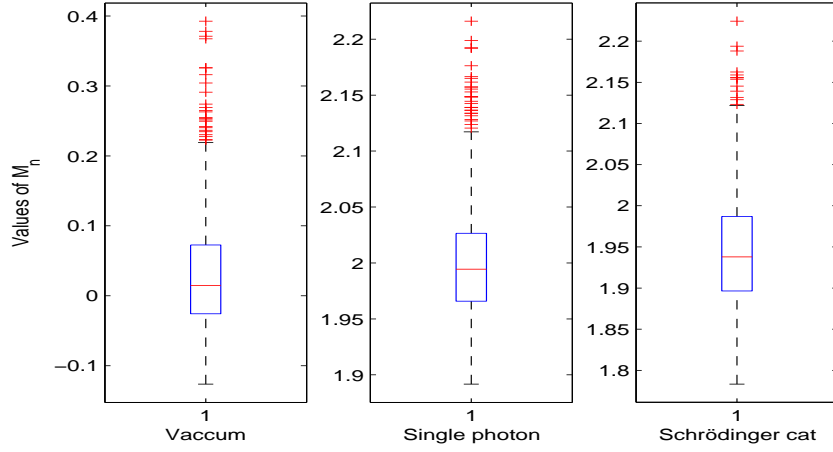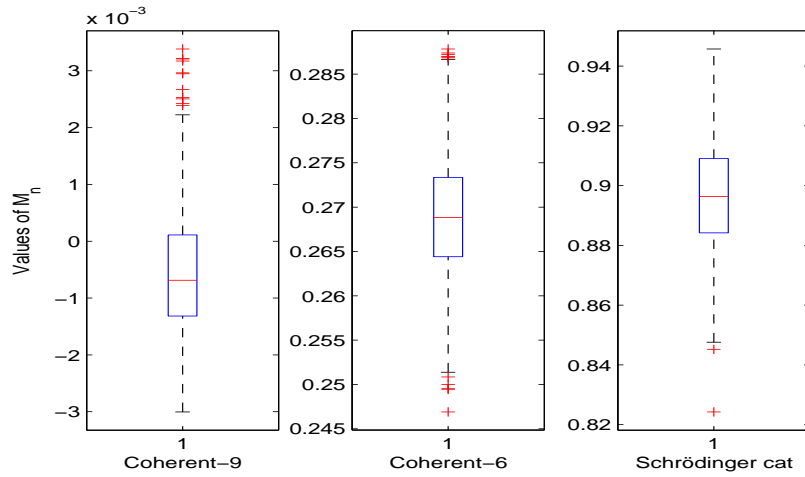

Figure 9: Case **B** τ is the *coherent*-3 state: **a)** ρ the *coherent*-3 state, **b)** ρ the *coherent*-$\sqrt{6}$ state and **c)** ρ the *Schrödinger cat* state for $\eta = 1$, $N = 15$

Figure 10: Case **B** τ is the *coherent*-3 state: **a)** ρ the *coherent*-3 state, **b)** ρ the *coherent*-$\sqrt{6}$ state and **c)** ρ the *Schrödinger cat* state for $\eta = 0.9$, $N = 14$

Figure 11: Case **B** τ is the *coherent*-3 state: **a)** ρ the *coherent*-3 state, **b)** ρ the *coherent*-$\sqrt{6}$ state and **c)** ρ the *Schrödinger cat* state for $\eta = 0.9$, $N = 13$
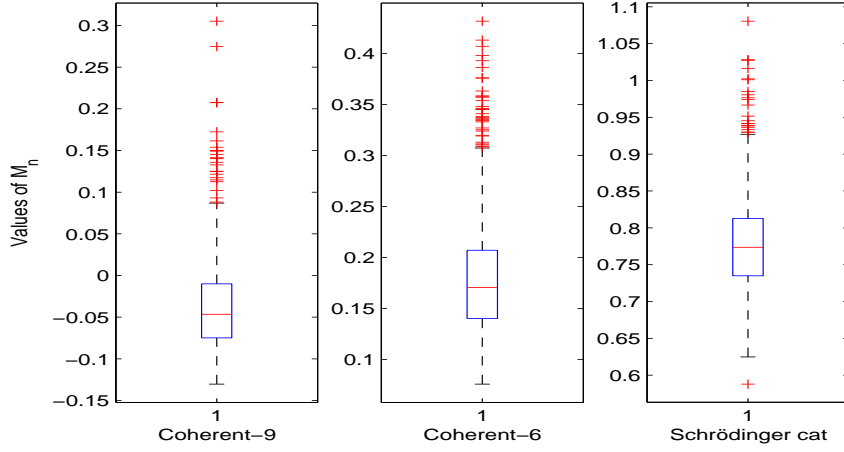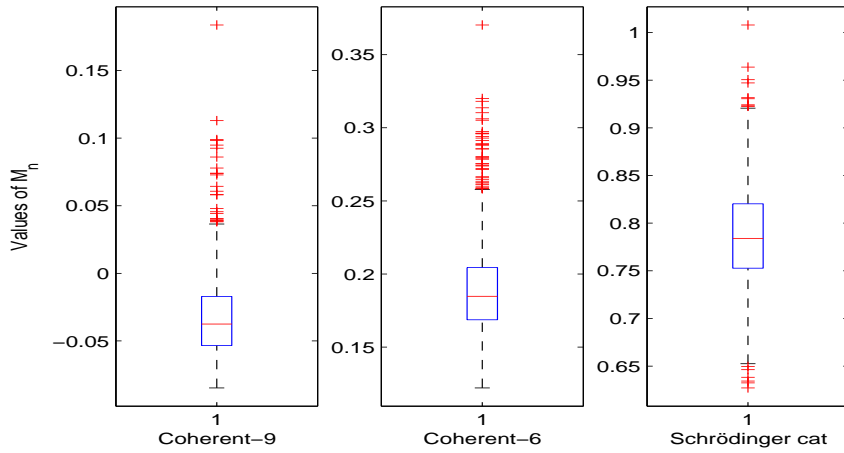
In order to evaluate the quality of our procedure M_n we compute the mean square error MSE $= E_\rho[|M_n - \|\rho - \tau\|_2^2|^2]$ as the average over $n_e = 1000$ independent runs of $|M_n - \|\rho - \tau\|_2^2|^2$, with $\|\rho - \tau\|_2^2$ given by Tables 2 and 3. Table 6 and 7 summarize the results. As we have already noticed the procedure M_n gives excellent results in every cases but it has a larger MSE when we evaluate the distance between the *coherent*-3 state and the *Schrödinger cat* state: MSE is equal to 0.0531 and 0.0484.

Table 6: The values of MSE for case **A**: τ the *vacuum* state

ρ	**a)** *vacuum*	**b)** *single photon*	**c)** *Schrödinger cat*
$N = 15, \eta = 1$	$2.3988 \cdot 10^{-5}$	$1.3175 \cdot 10^{-4}$	$4.7877 \cdot 10^{-4}$
$N = 14, \eta = 0.9$	0.0181	0.0056	0.0071
$N = 13, \eta = 0.9$	0.0069	0.0025	0.0051

Table 7: The values of MSE for case **B**: τ the *coherent*-3 state

ρ	**a)** *coherent*-3	**b)** *coherent*-$\sqrt{6}$	**c)** *Schrödinger cat*
$N = 15, \eta = 1$	$1.4303 \cdot 10^{-6}$	$1.9473 \cdot 10^{-4}$	0.0110
$N = 14, \eta = 0.9$	0.0044	0.0132	0.0531
$N = 13, \eta = 0.9$	0.0019	0.0093	0.0484

4.3 Studies of the performance of our test procedure Ω_n

In this part, we would like to confirm the performance of our testing procedure Ω_n. In order to appreciate it, we recall that the *power* of the test is the probability to correctly reject the false null hypothesis. We denote π_n the *power* of the test and defined it as follows:

$$\pi_n = P_\rho[\Omega_n = 1] = P_\rho[|M_n| > \mathcal{C}^* t_n^2] \quad \text{under } \rho \text{ satisfying } H_1(\mathcal{C}, \varphi_n).$$

Independently of the future runs, we first compute the estimator M_n as described in previous sections and we would like to compare it with a threshold t_n. We decide as follows. If $|M_n| > t_n(\alpha)$ we accept H_1, otherwise we accept H_0. In the statistical literature, the parameter $t_n = t_n(\alpha)$ is also called the critical value associated to α, which is the probability error of first type and defined as follows:

$$P_\tau[\Omega_n = 1] = P_\tau\left[|M_n| > \mathcal{C}^* t_n^2\right] = \alpha.$$

In our framework, we set $\alpha = 1\%$ and $\alpha = 5\%$.

As we don't know the density probability of M_n under $\rho = \tau$ defined in H_0, we shall evaluate empirically the threshold t_n at the testing level α for our particular choices of τ, $n = 50000$, α and η. In this purpose, we run $n_e = 1000$ iterations of M_n, each independently computed as described in the beginning of Section 4. We summarize our results in Table 8. We report that the obtained values t_n are larger when $\eta = 0.9$ than when $\eta = 1$. It is due to the noise effect.

Table 8: Values of t_n

	Case **A** : τ the *vacuum*	Case **B** : τ the *coherent*-3
$N = 15, \eta = 1$	$t_n(1\%) = 0.0096$	$t_n(1\%) = 0.0028$
	$t_n(5\%) = 0.0079$	$t_n(5\%) = 0.0022$
$N = 14, \eta = 0.9$	$t_n(1\%) = 0.4605$	$t_n(1\%) = 0.1453$
	$t_n(5\%) = 0.2739$	$t_n(5\%) = 0.1100$
$N = 13, \eta = 0.9$	$t_n(1\%) = 0.2692$	$t_n(1\%) = 0.0798$
	$t_n(5\%) = 0.1666$	$t_n(5\%) = 0.0713$

From now on, we fix the value of t_n as in Table 8. With the same protocol as above, we run independently of the previous runs $n_r = 1000$ independent replications of M_n, each independently computed as described previously. Hence, we evaluate the empirical power of our testing procedure and the empirical first type error. Tables 9 and 10 provide the empirical results obtained by our test procedure in the experiments

we deal with. We see that our testing procedure provides very good results even in the framework $\mathbf{B}$, we obtain powers π_n equal to 1 since $N = 13$ when we are in presence of noise. Otherwise, for $N = 14$ and $\eta = 0.9$ the powers of our testing procedure is a little bit degraded since $\pi_n = 0.7160$ for $\alpha = 1\%$ and $\pi_n = 0.9440$ for $\alpha = 5\%$ in the framework $\mathbf{B}$ when ρ is the *coherent-*$\sqrt{6}$ state, the optimal N when we are in presence of noise is $N = 13$ with powers of test equal to 1.

Table 9: Case $\mathbf{A}$- τ *vacuum*: empirical values of the first type error α and the power of the test π_n over 1000 runs for t_n given in Table 8

ρ	**a)** *vacuum*	**b)** *single ph.*	**c)** *Schrödinger C.*
	α	π_n	π_n
$N = 15, \eta = 1, t_n(1\%)$	0.0150	1.0000	1.0000
$N = 15, \eta = 1, t_n(5\%)$	0.0570	1.0000	1.0000
$N = 14, \eta = 0.9, t_n(1\%)$	0.0070	1.0000	1.0000
$N = 14, \eta = 0.9, t_n(5\%)$	0.0550	1.0000	1.0000
$N = 13, \eta = 0.9, t_n(1\%)$	0.0130	1.0000	1.0000
$N = 13, \eta = 0.9, t_n(5\%)$	0.0680	1.0000	1.0000

Table 10: Case **B**- τ *coherent*-3: empirical values of the first type error α and the power of the test π_n over 1000 runs for t_n given in Table 8

ρ	**a)** *coherent*-3	**b)** *coherent*-$\sqrt{6}$	**c)** *Schrödinger C.*
	α	π_n	π_n
$N = 15, \eta = 1, t_n(1\%)$	0.0090	1.0000	1.0000
$N = 15, \eta = 1, t_n(5\%)$	0.0530	1.0000	1.0000
$N = 14, \eta = 0.9, t_n(1\%)$	0.0120	0.7160	1.0000
$N = 14, \eta = 0.9, t_n(5\%)$	0.0680	0.9440	1.0000
$N = 13, \eta = 0.9, t_n(1\%)$	0.0230	1.0000	1.0000
$N = 13, \eta = 0.9, t_n(5\%)$	0.0620	1.0000	1.0000

5 Proof

In this last section, we give the proofs of the Theorem 1 and Theorem 2 derived in Section 3.3 and the proofs of the Proposition 1 and 2 established in Section 3.2.

5.1 Proof of the Theorems

In the paragraphs below, we establish the results of the Theorem 1 and 2 derived in Section 3.3. We begin by Theorem 1-(1).

Proof of Theorem 1-(1). Take $r \in]0, 2]$, $\eta = 1$, the bandwidth N_1 defined in the equation (15) and φ_n^2 defined in (16), we have by Proposition 2-2 and Proposition 2-1

$$V_\tau(M_n) \leq \frac{(C \cdot C_2)^2}{n^2} N_1^{17/3} \leq C_{V_\tau} \varphi_n^8, \tag{21}$$

$$V_\rho(M_n) \leq \frac{8C \cdot C_2}{n} N_1^{17/6} \leq C_V \varphi_n^4, \tag{22}$$

where C_V and C_{V_τ} are positive constants depending only on B, r and L.

Under $\rho = \tau$ defined in H_0, from Proposition 1, equations (21) and (16), we

bound from above the first type error as follows:

$$P_\tau[\Omega_n = 1] = P_\tau \left[|M_n| \geq \mathcal{C}^* t_n^2 \right] \leq \frac{E_\tau[|M_n|^2]}{\mathcal{C}^{*2} t_n^4} = \frac{V_\tau[M_n]}{\mathcal{C}^{*2} t_n^4} \leq \frac{C_{V_\tau} \varphi_n^4}{\mathcal{C}^{*2}} \to 0,$$

as $n \to \infty$.

On the other hand, under ρ satisfying $H_1(\mathcal{C}, \varphi_n)$, we have the second type error bounded as follows:

$$P_\rho[\Omega_n = 0] = P_\rho \left[|M_n| < \mathcal{C}^* t_n^2 \right]$$
$$\leq P_\rho \left[|M_n - E_\rho[M_n]| \geq \|\rho - \tau\|^2 - \mathcal{C}^* t_n^2 - B_\rho[M_n] \right].$$

Moreover, under ρ satisfying $H_1(\mathcal{C}, \varphi_n)$, let $\mathcal{C} = \mathcal{C}^*(1 + \delta)$, $\delta \in]0, 1[$, Proposition 1, equations (26) and (20) imply that $B_\rho \leq \frac{\delta}{2} \mathcal{C}^* \varphi_n^2$ for n large enough and then

$$P_\rho[\Omega_n = 0] \leq P_\rho \left[\frac{|M_n - E_\rho[M_n]|}{\sqrt{V_\rho(M_n)}} \geq \frac{\|\rho - \tau\|^2 - \mathcal{C}^* t_n^2 - B_\rho[M_n]}{C_V \varphi_n^2} \right]$$
$$\leq P_\rho \left[\frac{|M_n - E_\rho[M_n]|}{\sqrt{V_\rho(M_n)}} \geq \frac{\delta \mathcal{C}^*/2}{\sqrt{C_V}} \right]$$
$$\leq \frac{4 C_V}{(\delta \mathcal{C}^*)^2} \leq \frac{\lambda}{2},$$

for $\mathcal{C}^*$ large enough. $\qquad\square$

Proof of Theorem 1-(2). For $r = 2$, $\eta \in]1/2, 1[$, the bandwidth N_2 defined in the equation (17) and φ_n^2 defined in (20), we know by Proposition 2-2 and Proposition 2-1 that

$$V_\tau(M_n) \leq \frac{(\mathcal{C}_\infty^\eta)^2}{n^2} N_2^{-4/3} e^{32\gamma N_2} \leq C'_{V_\tau} \varphi_n^8, \tag{23}$$

$$V_\rho(M_n) \leq \frac{8 \mathcal{C}_\infty^\eta}{n} N_2^{-2/3} e^{16\gamma N_2} \leq C'_V \varphi_n^4, \tag{24}$$

where C'_V and C'_{V_τ} are positive constants depending only on B, r, L and η.

On one hand, under $\rho = \tau$ defined in H_0, by Proposition 1, equations (23) and (18), we have the first type error bounded as follows:

$$P_\tau[\Omega_n = 1] = P_\tau \left[|M_n| \geq \mathcal{C}^* t_n^2\right] \leq \frac{E_\tau[|M_n|^2]}{\mathcal{C}^{*2} t_n^4}$$

$$= \frac{V_\tau[M_n]}{\mathcal{C}^{*2} t_n^4} \leq \frac{C'_{V_\tau} \varphi_n^4}{\mathcal{C}^{*2}} \to 0,$$

as $n \to \infty$.

On the other hand, under ρ satisfying $H_1(\mathcal{C}, \varphi_n)$, the second type error is bounded as follows:

$$P_\rho[\Omega_n = 0] = P_\rho \left[|M_n| < \mathcal{C}^* t_n^2\right]$$

$$\leq P_\rho \left[|M_n - E_\rho[M_n]| \geq \|\rho - \tau\|^2 - \mathcal{C}^* t_n^2 - B_\rho[M_n]\right].$$

From Proposition 1, equations (24) and (18), since we are under ρ satisfying $H_1(\mathcal{C}, \varphi_n)$, we get

$$P_\rho[\Omega_n = 0] \leq P_\rho \left[\frac{|M_n - E_\rho[M_n]|}{\sqrt{V_\rho(M_n)}} \geq \frac{\|\rho - \tau\|^2 - \mathcal{C}^* t_n^2 - B_\rho[M_n]}{C'_V \varphi_n^2}\right]$$

$$\leq P_\rho \left[\frac{|M_n - E_\rho[M_n]|}{\sqrt{V_\rho(M_n)}} \geq \frac{\mathcal{C} - \mathcal{C}^* - C_B}{\sqrt{C'_V}}\right]$$

$$\leq \frac{C'_V}{(\mathcal{C} - \mathcal{C}^* - C_B)^2} \leq \frac{\lambda}{2},$$

for $\mathcal{C} > \mathcal{C}^*$ and $\mathcal{C}^*$ large enough. $\qquad \square$

Proof of Theorem 2. In the case $r \in]0, 2[$ and $\eta \in]1/2, 1[$, for the bandwidth N_3 solution of the equation (19) and for φ_n^2 defined in (20), Proposition 2-2 and Proposition 2-1 give that

$$V_\tau(M_n) \leq \frac{(\mathcal{C}_\infty^\eta)^2}{n^2} N_3^{-4/3} e^{32\gamma N_3} \leq C''_{V_\tau} \varphi_n^8 \cdot N_3^{\frac{2(3r-14)}{3}} \leq C''_{V_\tau} \varphi_n^8 \tag{25}$$

$$V_\rho(M_n) \leq \frac{8\mathcal{C}_\infty^\eta}{n} N_3^{-2/3} e^{16\gamma N_3} \leq C''_V \varphi_n^4 \cdot N_3^{\frac{3r-14}{3}} \tag{26}$$

where C''_V and C''_{V_τ} are positive constants depending only on B, r, L and η.

31

Under $\rho = \tau$ defined in H_0, from Proposition 1, equations (25) and (20), it follows that the first type error satisfies

$$P_\tau[\Omega_n = 1] = P_\tau\left[|M_n| \geq \mathcal{C}^* t_n^2\right] \leq \frac{E_\tau[|M_n|^2]}{\mathcal{C}^{*2} t_n^4} = \frac{V_\tau[M_n]}{\mathcal{C}^{*2} t_n^4} \leq \frac{C_{V_\tau}'' \varphi_n^4}{\mathcal{C}^{*2}} \to 0,$$

as $n \to \infty$.

Furthermore, under ρ satisfying $H_1(\mathcal{C}, \varphi_n)$, the second type error is such that

$$
\begin{aligned}
P_\rho[\Omega_n = 0] &= P_\rho\left[|M_n| < \mathcal{C}^* t_n^2\right] \\
&\leq P_\rho\left[|M_n - E_\rho[M_n]| \geq \|\rho - \tau\|^2 - \mathcal{C}^* t_n^2 - B_\rho[M_n]\right].
\end{aligned}
$$

From Proposition 1, equations (26) and (20), since we are under ρ satisfying $H_1(\mathcal{C}, \varphi_n)$, we deduce that

$$P_\rho[\Omega_n = 0] \leq P_\rho\left[\frac{|M_n - E_\rho[M_n]|}{\sqrt{V_\rho(M_n)}} \geq \frac{\mathcal{C} - \mathcal{C}^* - C_B}{\sqrt{C_V''} N_3^{\frac{3r-14}{6}}}\right] \leq \frac{C_V'' N_3^{\frac{3r-14}{3}}}{(\mathcal{C} - \mathcal{C}^* - C_B)^2} \to 0,$$

as $n \to \infty$, for $\mathcal{C} > \mathcal{C}^*$ and $\mathcal{C}^*$ large enough. $\qquad\square$

5.2   Proof of the Propositions

In the following paragraphs, we give the proofs of the Proposition 1 and 2 established in Section 3.2.

Proof of Proposition 1. By Remark 1, for $r \in\,]0, 2]$

$$B_\rho(M_n) = \left|E_\rho[M_n] - \|\rho - \tau\|_2^2\right| = \left|E_\rho[M_n] - \sum_{j,k \geq 0} |\rho_{j,k} - \tau_{j,k}|^2\right|.$$

It is easy to see that under $\rho = \tau$ defined in H_0, we have $B_\tau(M_n) = 0$. Under ρ satisfying $H_1(\mathcal{C}, \varphi_n)$,

$$B_\rho(M_n) = \left| \sum_{j,k=0}^{N-1} |\rho_{j,k} - \tau_{j,k}|^2 - \sum_{j,k \geq 0} |\rho_{j,k} - \tau_{j,k}|^2 \right|$$

$$= 2 \sum_{j=N}^{\infty} \sum_{k=0}^{j-1} |\rho_{j,k} - \tau_{j,k}|^2 + \sum_{j=N}^{\infty} |\rho_{j,j} - \tau_{j,j}|^2$$

$$\leq 4 \sum_{j=N}^{\infty} \sum_{k=0}^{j-1} \left(|\rho_{j,k}|^2 + |\tau_{j,k}|^2 \right) + 2 \sum_{j=N}^{\infty} \left(|\rho_{j,j}|^2 + |\tau_{j,j}|^2 \right)$$

Since τ and ρ belong to the class $\mathcal{R}(B, r, L)$ defined in (6), it implies

$$B_\rho(M_n) \leq 8L^2 \sum_{j=N}^{\infty} \sum_{k=0}^{j-1} e^{-2B(j+k)^{r/2}} + 4L^2 \sum_{j=N}^{\infty} e^{-2B(j+j)^{r/2}}$$

$$\leq 8L^2 \int_N^{\infty} (j-1) e^{-2Bu^{r/2}} du + 4L^2 \int_N^{\infty} e^{-2B(2u)^{r/2}} du$$

$$\leq C_B N^{2-r/2} e^{-2BN^{r/2}} + C_B' N^{1-r/2} e^{-2B(2N)^{r/2}},$$

where C_B and C_B' denote positive constants depending only on B, r and L. As $2^{r/2} > 1$ for all $r > 0$,

$$B_\rho(M_n) \leq C_B N^{2-r/2} e^{-2BN^{r/2}} (1 + o(1)),$$

as $N \to \infty$. $\qquad\qquad\qquad\qquad\qquad\qquad\qquad\qquad\qquad\qquad\qquad$ $\square$

Proof of Proposition 2. By centering variables, we have $M_n - E_\rho[M_n] := F_1 + F_2$ where

$$F_1 := \frac{1}{n(n-1)} \sum_{j,k=0}^{N-1} \sum_{\ell \neq m=1}^{n} \left(F_{j,k}^\eta \left(\frac{Y_\ell}{\sqrt{\eta}}, \Phi_\ell \right) - E_\rho \left[F_{j,k}^\eta \left(\frac{Y}{\sqrt{\eta}}, \Phi \right) \right] \right)$$

$$\times \left(\overline{F_{j,k}^\eta} \left(\frac{Y_m}{\sqrt{\eta}}, \Phi_m \right) - E_\rho \left[\overline{F_{j,k}^\eta} \left(\frac{Y}{\sqrt{\eta}}, \Phi \right) \right] \right)$$

$$F_2 := \frac{2}{n} \sum_{j,k=0}^{N-1} \sum_{\ell=1}^{n} \mathcal{R}\mathrm{e} \left(\left(F_{j,k}^\eta \left(\frac{Y_\ell}{\sqrt{\eta}}, \Phi_\ell \right) - E_\rho \left[F_{j,k}^\eta \left(\frac{Y}{\sqrt{\eta}}, \Phi \right) \right] \right) \right.$$

$$\left. \times E_\rho \left[\overline{F_{j,k}^\eta} \left(\frac{Y}{\sqrt{\eta}}, \Phi \right) - \overline{\tau_{j,k}} \right] \right)$$

where $\mathcal{R}e(z)$ stands for the real part of the complex number z.

Then, $V_\rho(M_n) := E_\rho\left[|M_n - E_\rho\left[|M_n|\right]|^2\right] = E_\rho\left[|F_1|^2\right] + E_\rho\left[|F_2|^2\right]$. First deal with the first term of the previous sum $E_\rho\left[|F_1|^2\right]$

$$E_\rho\left[|F_1|^2\right] = \frac{1}{n(n-1)}E_\rho\left[\left|\sum_{j,k=0}^{N-1}\left(F_{j,k}^\eta\left(\frac{Y_1}{\sqrt{\eta}},\Phi_1\right) - E_\rho\left[F_{j,k}^\eta\left(\frac{Y}{\sqrt{\eta}},\Phi\right)\right]\right)\right.\right.$$

$$\left.\left.\left(\overline{F_{j,k}^\eta}\left(\frac{Y_2}{\sqrt{\eta}},\Phi_2\right) - E_\rho\left[\overline{F_{j,k}^\eta}\left(\frac{Y}{\sqrt{\eta}},\Phi\right)\right]\right)\right|^2\right].$$

By the Cauchy-Schwarz inequality on the sum and as $E[|X - E[X]|^2] \leq E[|X|^2]$:

$$E_\rho\left[|F_1|^2\right] \leq \frac{1}{n^2}\left(\sum_{j,k=0}^{N-1}E_\rho\left[\left|F_{j,k}^\eta\left(\frac{Y}{\sqrt{\eta}},\Phi\right)\right|^2\right]\right)^2.$$

A direct consequence of Remark 2 is

$$E_\rho\left[|F_1|^2\right] \leq \begin{cases} \frac{(\mathcal{C}_\infty^\eta)^2}{n^2}N^{-4/3}e^{32\gamma N} & \text{for } \eta \in]1/2, 1[, \\ \frac{(C\cdot\mathcal{C}_2)^2}{n^2}N^{17/3} & \text{for } \eta = 1. \end{cases}$$

By noticing $|\mathcal{R}e(z)| \leq |z|$, the second term of the sum $E_\rho\left[F_2^2\right]$ is such that

$$E_\rho\left[|F_2|^2\right] \leq \frac{4}{n}E_\rho\left[\left|\sum_{j,k=0}^{N-1}\left(F_{j,k}^\eta\left(\frac{Y_1}{\sqrt{\eta}},\Phi_1\right) - E_\rho\left[F_{j,k}^\eta\left(\frac{Y}{\sqrt{\eta}},\Phi\right)\right]\right)\right.\right.$$

$$\left.\left.\times\ E_\rho\left[F_{j,k}^\eta\left(\frac{Y}{\sqrt{\eta}},\Phi\right) - \tau_{j,k}\right]\right|^2\right]$$

By the Cauchy-Schwarz inequality on the sum and as $E[|X - E[X]|^2] \leq E[|X|^2]$:

$$E_\rho\left[|F_2|^2\right] \leq \frac{4}{n}\left(\sum_{j,k=0}^{N-1}E_\rho\left[\left|F_{j,k}^\eta\left(\frac{Y}{\sqrt{\eta}},\Phi\right)\right|^2\right]\right)$$

$$\times\left(\sum_{j,k=0}^{N-1}\left|E_\rho\left[F_{j,k}^\eta\left(\frac{Y}{\sqrt{\eta}},\Phi\right)\right] - \tau_{j,k}\right|^2\right)$$

$$\leq \frac{4}{n}\|\rho - \tau\|_2^2\left(\sum_{j,k=0}^{N-1}E_\rho\left[\left|F_{j,k}^\eta\left(\frac{Y}{\sqrt{\eta}},\Phi\right)\right|^2\right]\right)$$

By Remark 2 and as $\|\rho\|_2^2$, $\|\tau\|_2^2 \leq 1$ we obtain under ρ satisfying $H_1(\mathcal{C}, \varphi_n)$

$$E_\rho\left[|F_2|^2\right] \leq \begin{cases} \frac{8\mathcal{C}_\infty^\eta}{n} N^{-2/3} e^{16\gamma N} & \text{for } \eta \in]1/2, 1[, \\ \frac{8C \cdot \mathcal{C}_2}{n} N^{17/6} & \text{for } \eta = 1. \end{cases}$$

If, N is such that the upper bound of $E_\rho\left[|F_2|^2\right]$ tends to 0 with n, then this is the dominant term in the upper bound of $V_\rho(M_n)$. In addition, notice that under $\rho = \tau$ defined in H_0, we have $E_\tau\left[|F_2|^2\right] = 0$. $\qquad\square$

References

[1] D. L. Allen. Hypothesis testing using an L_1-distance bootstrap. *The American Statistician*, 51(2):145–150, 1997.

[2] N. H. Anderson, P. Hall, and D. M. Titterington. Two-sample test statistics for measuring discrepancies between two multivariate probability density functions using kernel-based density estimates. *Journal of Multivariate Analysis*, 50(1):41–54, 1994.

[3] L. Artiles, R. Gill, and M. Guţǎ. An invitation to quantum tomography. *J. Royal Statist. Soc. B (Methodological)*, 67:109–134, 2005.

[4] J. M. Aubry, C. Butucea, and K. Meziani. State estimation in quantum homodyne tomography with noisy data. http://arxiv.org/abs/0804.2434, 2008.

[5] Y. Baraud. Non asymptotic minimax rates of testing in signal detection. *Bernoulli*, 8, 2002.

[6] P. J. Bickel and M. Rosenblatt. On some global measures of the deviations of density function estimates. *Annals of Statistics*, 1(6):1071–1095, 1973.

[7] G. Breitenbach, S. Schiller, and J. Mlynek. Measurement of the quantum state of the squeezed light. *Nature*, 387:471–475, 1997.

[8] C. Butucea. Goodness-of-fit testing and quadratic functional estimation from indirect observations. *The Annals of Statistics*, 35(5):1907–1930, 2007.

[9] C. Butucea, M. Guţă, and L. Artiles. Minimax and adaptive estimation of the Wigner function in quantum homodyne tomography with noisy data. *Ann. Statist.*, 35(2):465–494, 2007.

[10] G. M. D'Ariano. Tomographic measurement of the density matrix of the radiation field. *Quantum Semiclass. Optics*, 7:693–704, 1995.

[11] G. M. D'Ariano. Tomographic methods for universal estimation in quantum optics. In *International School of Physics Enrico Fermi*, volume 148. IOS Press, 2002.

[12] G. M. D'Ariano, U. Leonhardt, and H. Paul. Homodyne detection of the density matrix of the radiation field. *Phys. Rev. A*, 52:R1801–R1804, 1995.

[13] G. M. D'Ariano, C. Macchiavello, and M. G. A. Paris. Detection of the density matrix through optical homodyne tomography without filtered back projection. *Phys. Rev. A*, 50:4298–4302, 1994.

[14] G.M. D'Ariano, L. Maccone, and M. F. Sacchi. Homodyne tomography and the reconstruction of quantum states of light. http://arxiv.org/abs/quant-ph/0507078, 2005.

[15] M. Fromont and B. Laurent. Adaptive goodness-of-fit tests in a density model. *Annals of Statistics*, 34(2), 2006.

[16] M. Guţă and L. Artiles. Minimax estimation of the Wigner in quantum homodyne tomography with ideal detectors. *Math. Methods Statist.*, 16(1):1–15, 2007.

[17] Y. I. Ingster and I. A. Suslina. *Nonparametric Goodness-of-fit Testing under Gaussian Models*. Lecture Notes in Statistics. Springer, 2003.

[18] U. Leonhardt. *Measuring the Quantum State of Light*. Cambridge University Press, 1997.

[19] U. Leonhardt, M. Munroe, T. Kiss, T. Richter, and M. G. Raymer. Sampling of photon statistics and density matrix using homodyne detection. *Opt. Commun.*, 127:144–160, 1996.

[20] U. Leonhardt, H. Paul, and G. M. D'Ariano. Tomographic reconstruction of the density matrix via pattern functions. *Phys. Rev. A*, 52:4899–4907, 1995.

[21] O. V. Lepski and A. B. Tsybakov. Asymptotically exact nonparametric hypothesis testing in sup-norm and at a fixed point. *Probab. Theory Related Fields*, 117(1):17–48, 2000.

[22] K. Meziani. Nonparametric estimation of the purity of a quantum state in quantum homodyne tomography with noisy data. *Mathematical Methods of Statistics*, 16(4):1–15, 2007.

[23] Y. Nikitin. *Asymptotic Efficiency of Nonparametric Tests*. Cambridge University Press, 1995.

[24] M. Nussbaum and A. Szkola. A lower bound of Chernoff type for symmetric quantum hypothesis testing. *to appear in Ann. Statist.*, 2008. http://arxiv.org/abs/quant-ph/0607216v1.

[25] A. Ourjoumtsev, R. Tualle-Brouri, J. Laurat, and P. Grangier. Generating optical Schrödinger kittens for quantum information processing. *Science*, 312(5770):83–86, 2006.

[26] C. Pouet. On testing nonparametric hypotheses for analytic regression functions in Gaussian noise. *Math. Methods Statist.*, 8(4):536–549 (2000), 1999.

[27] T. Richter. Pattern functions used in tomographic reconstruction of photon statistics revisited. *Phys. Lett. A*, 211:327–330, 1996.

[28] T. Richter. Realistic pattern functions for optical homodyne tomography and determination of specific expectation values. *Physical Review A*, 61(063819), 2000.

[29] D. T. Smithey, M. Beck, M. G. Raymer, and A. Faridani. Measurement of the Wigner distribution and the density matrix of a light mode using optical homodyne tomography: Application to squeezed states and the vacuum. *Phys. Rev. Lett.*, 70:1244–1247, 1993.

[30] V. G. Spokoiny. Adaptive hypothesis testing using wavelets. *Annals of Statistics*, 24(6), 1996.